Implementation of cell-free biological networks at steady state

Henrike Niederholtmeyer, Viktoria Stepanova, and Sebastian J. Maerkl[1]

Institute of Bioengineering, School of Engineering, École Polytechnique Fédérale de Lausanne, CH-1015 Lausanne, Switzerland

Edited by Jack W. Szostak, Howard Hughes Medical Institute and Massachusetts General Hospital, Boston, MA, and approved August 27, 2013 (received for review June 12, 2013)

Living cells maintain a steady state of biochemical reaction rates by exchanging energy and matter with the environment. These exchanges usually do not occur in in vitro systems, which consequently go to chemical equilibrium. This in turn has severely constrained the complexity of biological networks that can be implemented in vitro. We developed nanoliter-scale microfluidic reactors that exchange reagents at dilution rates matching those of dividing bacteria. In these reactors we achieved transcription and translation at steady state for 30 h and implemented diverse regulatory mechanisms on the transcriptional, translational, and posttranslational levels, including RNA polymerases, transcriptional repression, translational activation, and proteolysis. We constructed and implemented an in vitro genetic oscillator and mapped its phase diagram showing that steady-state conditions were necessary to produce oscillations. This reactor-based approach will allow testing of whether fundamental limits exist to in vitro network complexity.

synthetic biology | cell-free protein synthesis | computational biology | minimal artificial cell

Instead of complex and ill-characterized cellular hosts, in vitro systems have recently become popular alternatives for implementing synthetic networks. In vitro systems can be completely defined, easily manipulated, interrogated, and have been used to study a number of biological phenomena. For example, periodic temporal patterns were observed in systems based on nucleic acid synthesis and degradation (1, 2), and ordered spatial patterns were created from purified cell division regulators (3). In vitro transcription and translation (ITT)-based systems should, in principle, be able to use all regulatory functionalities found in living cells. Reconstituted, defined ITT systems like the PURE mix (4), are particularly appealing for bottom-up synthetic biology. A number of recent examples show that various genetic (5–10) and metabolic (11) networks can be implemented in ITT systems. Genetic network complexity has, however, been limited to genetic cascades, where the output of one stage acts on the next stage, whereas examples of positive and negative feedback have been basic (8, 9, 12). The main limitation to network complexity in vitro derives from its batch reaction format. In batch, synthesis rates decrease as precursors are consumed, enzymatic activities degrade, and reaction products accumulate. This rapid approach to chemical equilibrium severely limits network size. In addition, negative feedback is particularly difficult to implement, because regulators from earlier stages are not removed. The implementation of active degradation mechanisms for RNA and proteins (13) could solve the problem of product removal, and synthesis times can be increased by using reactors that allow an exchange of small molecules between the ITT mix and a feeding solution. Large-volume continuous flow and exchange systems were developed to increase the amounts of protein produced by ITT systems and are based on diffusion of small molecules through ultrafiltration membranes (14, 15). Scaled down versions of reactors using similar principles were more recently developed to increase throughput and minimize cost (16, 17). Cell-free genetic networks have, however, not yet profited from the full potential of continuous reaction conditions, although protein synthesis in a functionalized phospholipid vesicle surrounded by a feeding solution (18) and a two-stage genetic activation cascade in a dialysis system yielded promising results (9).

Results

Steady-State Transcription and Translation in Microfluidic Nanoreactors. To enable the implementation of complex genetic networks in vitro, we developed a microfluidic device in which ITT proceeds at steady state for extended periods of time. Our microfluidic device contains eight independent 33-nL reactors (*SI Appendix*) and functions similarly to previous devices (19–21). Dilutions occurred in discrete steps, where each dilution step added fresh ITT mix and template DNA, displacing part of the old reaction volume (Fig. 1*A*). Dilution rates could be precisely tuned by changing the volume displaced per dilution step in a range of 10–40% of reactor volume. The time interval between dilution steps was kept constant at 15 min (*SI Appendix*). These exchanges resulted in dilution rates of 0.4–2 h^{-1}. To enable long-term reactions, we cooled the ITT mix off chip to 6 °C, while keeping the on-chip reaction temperature at 37 °C. Fluorescent reporters allowed us to determine DNA, mRNA, and protein concentrations in real time (22) and a computer program controlled all device and imaging operations (Fig. 1*B* and *SI Appendix*).

We used a reaction rate model to describe the process of transcription and translation (22–24). We measured the reaction rate parameters that characterize an ITT batch reaction and added the dilution steps that replace fractions of the reactor volume with new reaction mix with full synthesis activity (Fig. 1*C*

Significance

Transcription and translation can be performed in vitro, outside of cells, allowing the assembly of artificial genetic networks. This bottom-up approach to engineering biological networks in a completely defined and minimal environment is instructive to define the rules and limitations of network construction. It is, however, still challenging to implement complex genetic networks in vitro because the reactions are usually performed in a batch format, where reaction products accumulate and synthesis rates decline over time. Here, we addressed this problem by developing a microfluidic device to perform in vitro transcription and translation reactions in continuous mode, where synthesis rates stay constant. This allowed us to build and implement a genetic oscillator that showed sustained oscillations for extended periods of times.

Author contributions: H.N. and S.J.M. designed research; H.N. and V.S. performed research; H.N. and S.J.M. analyzed data; and H.N. and S.J.M. wrote the paper.

The authors declare no conflict of interest.

This article is a PNAS Direct Submission.

Freely available online through the PNAS open access option.

[1]To whom correspondence should be addressed. E-mail: sebastian.maerkl@epfl.ch.

This article contains supporting information online at www.pnas.org/lookup/suppl/doi:10.1073/pnas.1311166110/-/DCSupplemental.

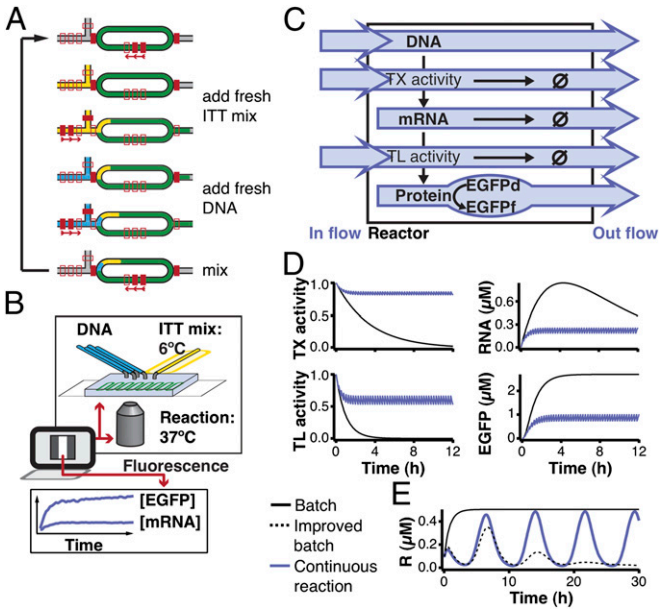

Fig. 1. ITT under steady-state conditions. (*A*) Function of a microfluidic nanoreactor for continuous ITT. At each dilution step, the supply channel is flushed with fresh reagent. A peristaltic pump meters a specific volume into the reaction ring. After both ITT mix and DNA have been added, another peristaltic pump mixes the reaction. (*B*) Experimental setup and analysis. (*C*) Model of EGFP synthesis in the reactor. Relative transcriptional (TX) and translational (TL) activities decrease at constant rates. In the continuous reaction (blue arrows), all modeled species are diluted at a constant rate, and DNA as well as relative TX and TL activities are replaced at the same rate. (*D*) Model predictions for a batch and a continuous reaction. Predictions were for 18.3 nM DNA and dilutions of 32% every 15 min. (*E*) Model of the repressilator (25) under three reaction conditions (*SI Appendix*). We show the concentration of one of the repressor proteins (R).

and *SI Appendix*). During continuous reaction, synthesis rates reach a steady state, where the rate at which activities decrease is balanced by the inflow rate of fresh reaction mix. Consequently, RNA and protein concentrations also reach steady-state levels (Fig. 1*D*). On the basis of our model, a genetic system such as the repressilator (25) would not oscillate in a batch reaction. Improvements like degradation mechanisms for mRNA and protein, as well as elongated synthesis times (9, 13, 18), could possibly lead to a few damped oscillations in batch, whereas sustained oscillations can only be obtained under continuous conditions (Fig. 1*E*).

We performed protein synthesis reactions in vitro, generating EGFP from a linear DNA template regulated by a T7 promoter at dilution rates comparable to bacterial doubling times between 20 and 104 min (Fig. 2*A*). We achieved dilution-dependent steady-state mRNA and protein levels for 30 h (Fig. 2*B*). Independent of dilution rate, DNA template concentration remained constant in all conditions (*SI Appendix*, Fig. S1). When we momentarily stopped the flow of fresh reagents, RNA and protein concentrations increased and returned to their previous steady-state levels when dilution was resumed (Fig. 2*C*). To demonstrate the dynamic nature of synthesis and dilution, we switched between periods where DNA template or water was added (Fig. 2*D*). This led to continuously changing DNA template concentrations with RNA and protein concentrations oscillating with a slight delay. Our model accurately captured these dynamic changes.

Implementation of Regulatory Mechanisms. We implemented a number of regulators, acting transcriptionally, translationally, and posttranslationally, under steady-state conditions. We transiently expressed the regulators to allow comparison of RNA and protein concentration of the reporter in the presence and absence of the regulator in one experiment (Fig. 3). We implemented transcriptional activation by expressing T3 RNA polymerase (T3RNAP) or sigma factor 70 (σ^{70}) in the presence of the *Escherichia coli* RNAP core enzyme and EGFP under control of their respective promoters. Expression of either protein increased RNA concentration from undetectable levels to ~150 and 18 nM for T3RNAP and *E. coli* RNAP, respectively, and also increased EGFP concentration in the expected manner (Fig. 3*A*). Transcriptional repression by the transcriptional repressor TetR reduced transcription of promoters expressed by three different polymerases (T3, T7, and *E. coli* RNAP). Coexpression of *tetR* reduced RNA levels to 30%, 50%, and 40% of their unrepressed levels for T3, T7, and *E. coli* RNAP, respectively. These changes of mRNA concentration consequently led to a decrease in EGFP levels (Fig. 3*B*). We implemented translational activation using two regulator RNAs that were previously used in vivo to induce mRNA translation by transactivation and stop codon suppression (Fig. 3*C*) (26, 27). In transactivation, a transactivator RNA modifies mRNA secondary structure of a *cis*-repressed RNA, making the ribosomal binding site accessible (26). For stop codon suppression, we used the amber suppressor tRNA encoded by *supD* allowing read through of a UAG stop codon (27), which was located immediately after the start codon of the EGFP gene. Aminoacylation of the tRNA with serine required no additives to the ITT system as both enzyme and amino acid are present. These mechanisms led to an increase in EGFP concentration from undetectable levels to 14 and 35 nM, whereas RNA concentrations remained high in the presence and absence of the regulator RNA (expression of *supD* reduced RNA concentration by about 10–20%, Fig. 3*B*). To quantify the effect of both activators on translation of their respective reporter mRNAs, which were synthesized at different concentrations, we used the model of EGFP ITT to determine the ratio of observed to expected EGFP concentration for the measured mRNA concentration. According to this analysis, translation efficiency was 1.4% for transactivation and 2.8% for stop codon suppression (*SI Appendix*, Fig. S2). Finally, we successfully implemented protein degradation by reconstituting the ATP-dependent protease ClpXP (a large 700- to 800-kDa multisubunit complex) (28). Degradation of GFP targeted for recognition by AAA^+ proteases such as ClpXP has been shown in cell extracts, where these proteases are naturally present (13). Here, we functionally expressed the protease in vitro and showed that it specifically degraded EGFP fused with the ssrA degradation tag. In the presence of ClpXP, steady-state EGFPssrA concentration decreased by about 80% (Fig. 3*D*). Again, we calculated expected EGFP concentrations from the measured mRNA concentrations, which decreased when ClpX and ClpP were expressed, to determine if EGFP decrease was indeed caused by protein degradation. Only in the case of ssrA-tagged EGFP did we observe a significant decrease of observed to expected EGFP when both protease subunits were expressed (*SI Appendix*, Fig. S2).

An in Vitro Genetic Oscillator. Using three regulators from this toolbox, we built a genetic oscillator based on a positive feedback and delayed negative feedback architecture (1, 2) (Fig. 4*A*). In our oscillator network, T3RNAP induces its own expression, which constitutes the positive feedback loop. The same polymerase also transcribes the *supD* and *tetR* genes to produce amber suppressor tRNA and *tetR* mRNA, which can only be translated when the suppressor tRNA concentration is sufficiently high. TetR then represses transcription of the T3RNAP gene, which eventually stops its own synthesis. Citrine and cerulean fluorescent proteins allowed us to simultaneously monitor expression from the two promoters in the system. A model of this genetic network (*SI Appendix*) produced oscillations using parameter estimates for the regulators involved. Modeling of this

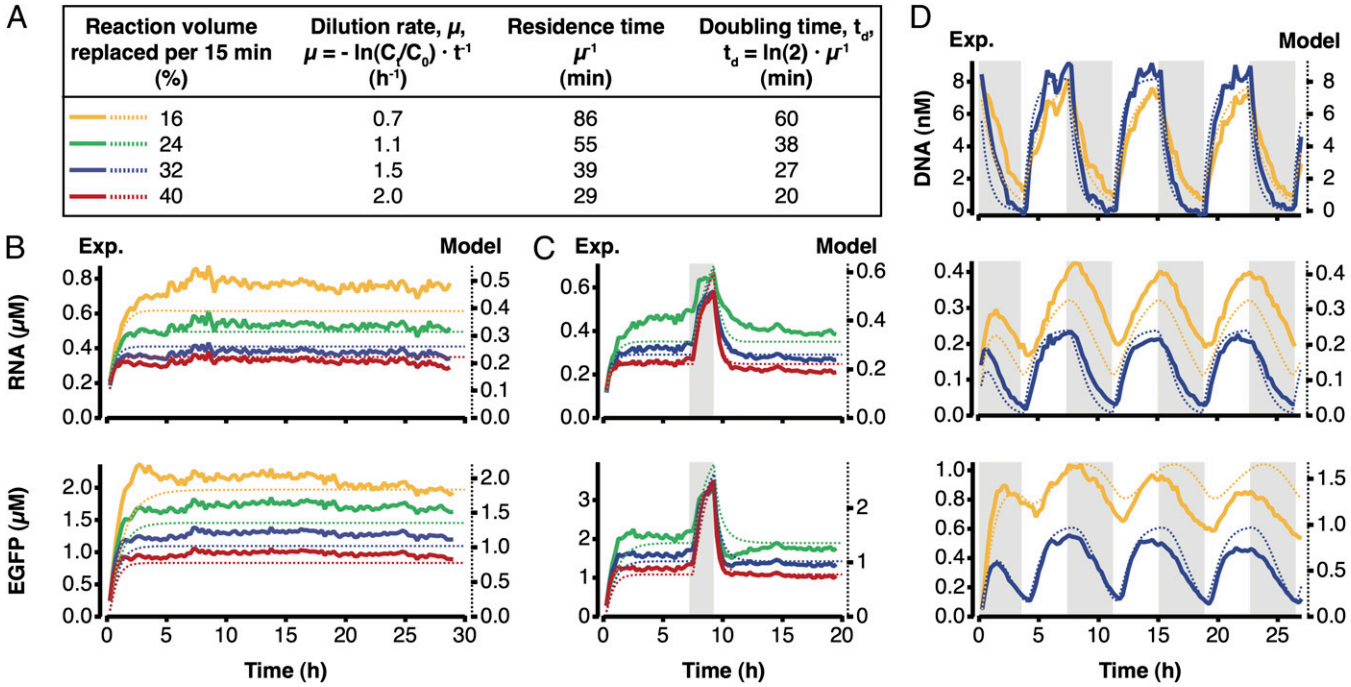

Fig. 2. Steady-state ITT. (*A*) Dilution conditions for the experiments in this figure. Experimental RNA and protein concentrations (solid lines, *Left* axes) and model prediction (dashed lines, *Right* axes) for (*B*) long-term ITT at different dilution rates, (*C*) a transient switch to batch conditions (shaded area), and (*D*) oscillating DNA template concentrations (shaded area, water added; white area, DNA added). DNA template concentration, 10 nM (*B* and *C*); maximum 8.2 nM (*D*).

system showed that the value of the dilution rate was critical for sustained oscillations to occur, which led us to test several dilution rates for each combination of DNA template concentrations. As expected, steady-state conditions were necessary to produce oscillations in our experiments and occurred only in a narrow range of dilution rates (Fig. 4*B*). The range of dilution rates that gave rise to oscillations increased with decreasing *supD* template concentration; *supD* was, however, necessary, as well as the other two components (*SI Appendix*, Fig. S3). For *supD* template concentrations below 82 nM, where oscillations were observed over a wider range of residence times, oscillation period increased linearly between 4 and 16 h as a function of residence time (*SI Appendix*, Fig. S4). These residence times correspond to cellular doubling times between 20 and 58 min. A similar dependence of period on dilution rate has been found for bacterial growth rates (29). Apart from oscillations or damped oscillations, two other general behaviors were observed: at high residence times reporter concentrations peaked once and then went to a low stable steady state, and at low residence times, or when *supD* template was absent, they immediately approached a stable steady state (Fig. 4*C* and *SI Appendix*, Fig. S5). The model of the oscillator produced similar results as a function of dilution rate (*SI Appendix*, Fig. S6) and was also able to capture the results of control experiments, where one network component at a time was removed from the system (*SI Appendix*, Figs. S3 and S7).

Discussion

Biological in vitro oscillations were previously achieved only in biochemically simple reactions, such as oligonucleotide-based systems containing an active degradation mechanism (1, 2). Our genetic oscillator shows that continuous reaction conditions allow complex dynamics to occur in cell-free protein synthesis reactions and in a sustained fashion. We observed that oscillations occurred in a narrow range of physiological dilution rates, which is important information for the implementation of in vivo oscillators, where dilution rates cannot be tuned as easily.

The examples of regulators we implemented in this study show that there appear to be no major limitations in the control mechanisms that can be implemented in vitro. Nonetheless, there are still many mechanisms to be tested, including different transcriptional repressors, transcriptional activators such as LuxR, or protein phosphorylation. Moreover, it may be possible to use systems that could not be implemented in vivo because of interference with vital processes in the host. In the course of characterizing different regulators with the goal of identifying suitable candidates to assemble a genetic oscillator, we found that *E. coli* RNA polymerase promoters recognized by σ^{70} often exhibited very low transcription rates. A recent report suggests that circular DNA might be a better template than linear DNA to reproduce in vivo transcription rates from *E. coli* promoters (30). To achieve tight repression of a strong promoter, we included two TetR operator sites into the T3 promoter, which explains its higher repression efficiency than the T7tet promoter. The TetR repressed version of the *E. coli* promoter featured two operator sites but the considerably lower activity in the unrepressed state made it less suitable for our oscillator design. The combination of transcriptional strength and tight repression are desirable features of promoters in many synthetic networks and often not trivial to engineer (25, 26). To achieve tighter control of the *tetR* gene in our oscillator network than transcriptional control could provide, we added stop codon suppression as a second regulatory level.

The reactor-based approach presented here allows bottom-up synthetic biology experiments to be performed in a completely defined and controlled environment. It differs from earlier designs of reactors for continuous ITT reactions (15, 17) in that it is not based on a size-exclusion membrane for exchange of molecules. In our microfluidic reactor-based approach, all molecules, including RNA polymerase, translation machinery, and DNA template, are constantly exchanged. Whereas the exchange

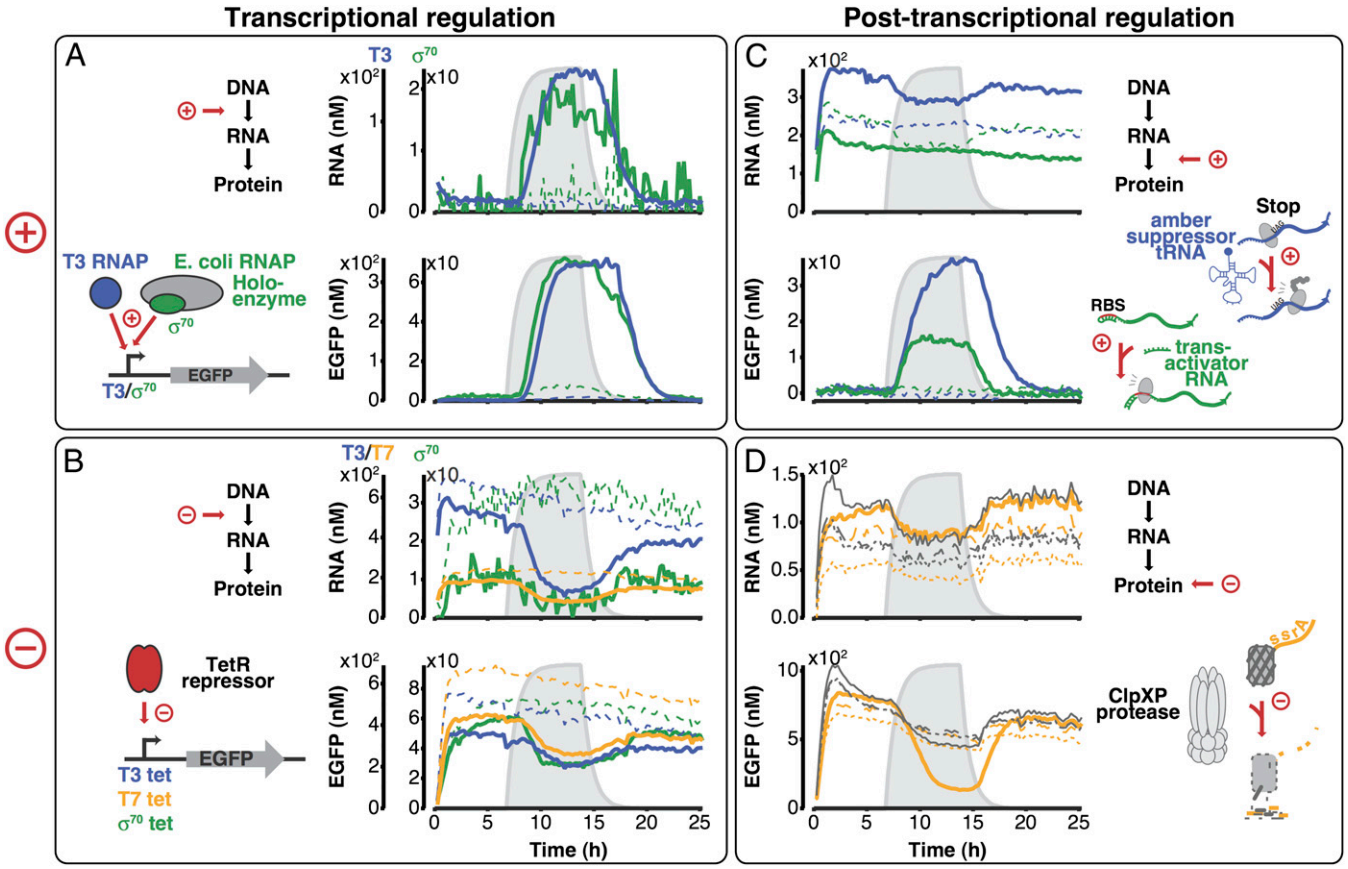

Fig. 3. Regulation at the transcriptional, translational, and posttranslational levels. Solid lines, experimental data; dashed lines, controls. DNA template of the regulator was transiently present (gray shaded area). Reporter (EGFP) DNA template was present at constant concentration. For a detailed summary of concentrations and controls, see *SI Appendix*, Table S2. (*A*) Transcriptional activation by T3RNAP and σ^{70}. *E. coli* RNAP core enzyme was present in the reaction mix. Controls: wrong activator. (*B*) Transcriptional repression by TetR. Promoters transcribed by three different RNA polymerases were tested in the presence of their respective polymerase. Controls: promoter without repressor binding site. (*C*) Activation of translation by RNA molecules. Controls: wrong activator. (*D*) Protein degradation by ClpXP protease. Controls: no degradation tag (ssrA), gray lines; only one protease subunit expressed, broken lines.

of enzymes involved in the reaction ensures that synthesis rates stay at a constant steady state even if they degrade over time, it could be interesting to immobilize the DNA templates in the reactor or to organize specific protein products in a spatial manner (31). Although our DNA template concentrations were in the range of low copy number plasmid concentrations in *E. coli*, RNA and protein concentrations were higher than average cellular concentrations. Due to the relatively large size of our nanoreactors (two orders of magnitude larger than the giant bacterium *Epulopiscium*) (32), stochastic processes may be difficult to study at the moment (33). It should however be feasible to scale down the 33-nL reactors by one to two orders of magnitude with existing microfabrication approaches (34) and to use *E. coil* RNAP instead of a phage RNAP. Down-scaling reactor volume would also permit hundreds to possibly thousands of reactors to be integrated on a single device (35, 36). Combined with high-throughput DNA synthesis methods (37) this approach would allow the rapid characterization of many synthetic network variants. Due to the fact that ITT reactions only require linear DNA templates, which were exclusively used in this study, such an in vitro screen would require no laborious cloning steps.

It will be exciting to determine whether any fundamental limits exist to the complexity of systems attainable in vitro. We were able to implement a genetic oscillator in vitro similar in complexity to synthetic gene networks achieved in vivo a few years ago (25). Our nanoreactor may prove to be a viable system to study processes that would interfere with vital processes in vivo or processes that occur in organisms that are unculturable. Furthermore, the system could be used to boot up and test the biochemical subsystems of a minimal artificial cell, including DNA replication (38), the translation machinery, or biosynthesis of precursors (39).

Methods

Preparation of DNA Templates. PCR for linear DNA templates was performed as previously described (22). Primer sequences are listed in *SI Appendix*, Table S1. PCR templates were pKT127 for EGFP (40), pKT211 for citrine (40), pBS10 for cerulean (Yeast Resource Center), BBa_K346000 (Registry of Standard Biological Parts) for T3 RNA polymerase, repressilator plasmid (25) for *tetR*, and *E. coli* DH5α genomic DNA for *rpoD*. Short DNA templates for *supD* (Registry of Standard Biological Parts; Part:BBa_K228001) and taR12 (26) were created by PCR using overlapping oligonucleotides. Regulatory sequences such as promoter, ribosomal binding site, terminator, and ssrA tag were included in the oligonucleotide primers. To monitor mRNA concentration, the EGFP template contained a target site for binary probes in its 3′ untranslated region (22). To monitor DNA concentration, the DNA template contained two Cy5 labels introduced by the 3′ and 5′ final primers.

Reaction Setup. We used the commercial PURExpress ITT kit (New England Biolabs) and added water to a volume of 80% of the final reaction volume. The remaining 20% of the reaction volume consisted of DNA template at five times its final concentration. ITT and DNA fractions were combined on the microfluidic chip. If necessary, the ITT mix was supplemented with binary probes (22) at a final concentration of 1 μM *E. coli* RNA polymerase core enzyme or holoenzyme (Epicenter) at 35 and 25 ng/μL, respectively, or 100 nM T3 RNAP polymerase (Fermentas). For a steady-state ITT reaction, ITT

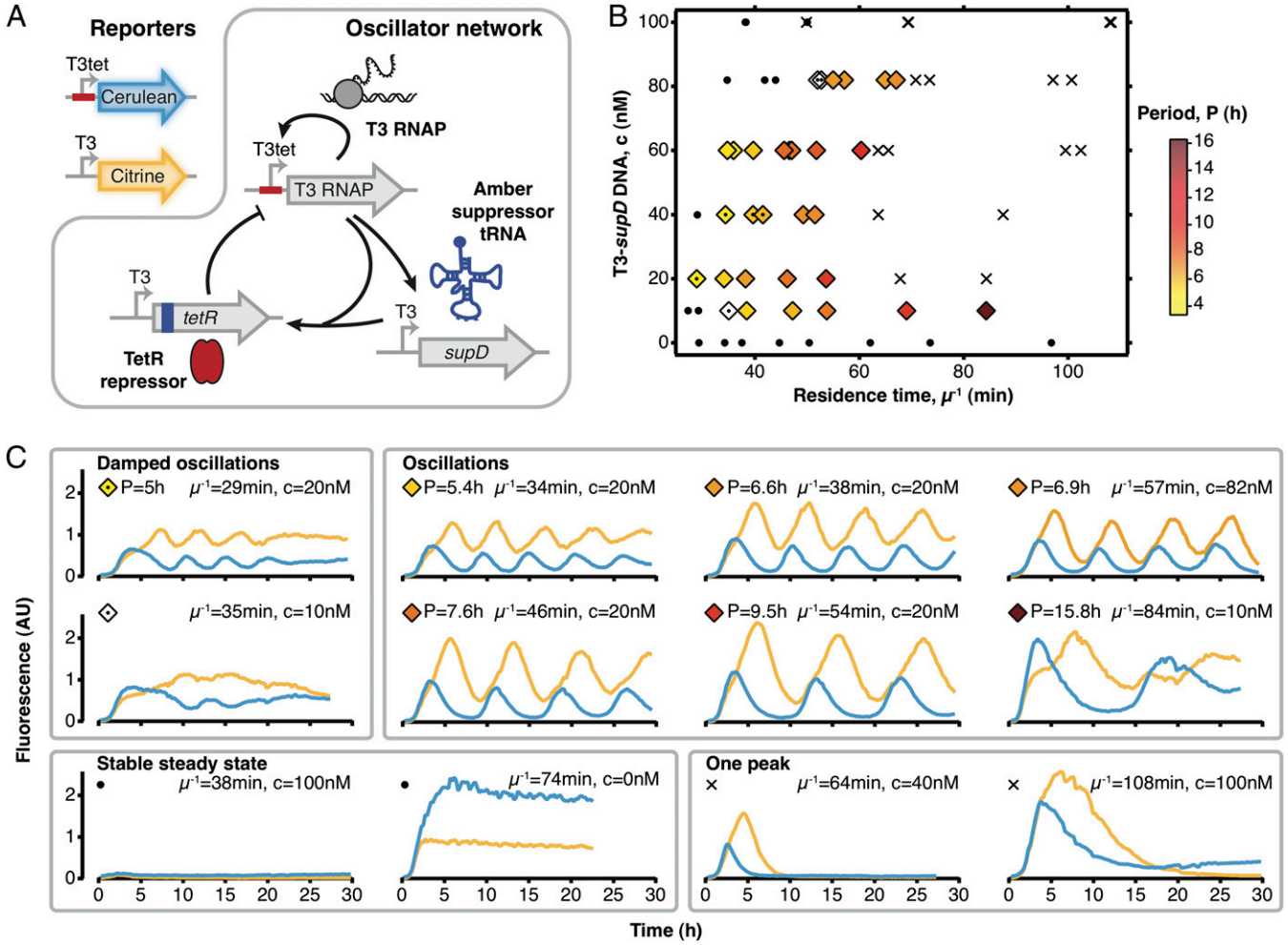

Fig. 4. Steady-state ITT conditions allow implementation of a genetic oscillator. (*A*) The oscillator network consists of three DNA templates: T3RNAP, *supD* amber suppressor tRNA, and TetR repressor. The TetR operator in the T3tet promoter and the amber stop codon in the *tetR* gene are indicated as red and blue boxes, respectively. Reporters for the two promoters in the network: yellow fluorescent protein (citrine) and cyan fluorescent protein (cerulean). (*B*) Phase diagram of the oscillator at different *supD* DNA template concentrations and different dilution rates. Oscillations (diamond symbols) occurred over a narrow range of dilution rates, which also determined the period of oscillations (fill color). Two other general behaviors were observed: one fluorescence peak and then low fluorescence (cross) or the system immediately reached a stable steady state (circles). (*C*) Cerulean (blue) and citrine (yellow) example traces.

mix and DNA were combined in the reactors on the microfluidic chip in a 5:1 ratio. Every 15 min, the reactor was imaged and a fraction of the reactor volume was replaced with fresh ITT mix and DNA at 5:1 ratio. Details on operation and characterization of the microfluidic chip can be found in the *SI Appendix*. Final concentrations of DNA templates in the genetic oscillator were 5 nM T3tet-T3RNAP, 10 nM T3-amber-*tetR*, and variable T3-*supD* concentration (between 0 and 100 nM). The reporter template DNAs for T3-citrine and T3-cerulean were at 2.5 nM each. Concentrations of DNA templates for the experiment with transcriptional and posttranscriptional regulators are summarized in *SI Appendix*, Table S2.

Data Acquisition and Analysis. We used an inverted microscope with an automated stage to image the eight reactors on the chip. Fluorescence was determined by imaging the reactor channel using a 20× magnification and fluorescence filters for GFP, Cy3-Cy5 FRET, Cy5, YFP, and CFP. Background fluorescence of a position next to the channel was subtracted from channel fluorescence. Concentrations of mRNA and EGFP were calculated from calibrations of FRET and EGFP fluorescence using purified molecules (22). To determine mRNA concentrations, we performed a blank reaction without DNA template in one of the reactors and subtracted FRET background fluorescence. Additionally, we normalized to average blank FRET fluorescence. To determine the period of sustained and damped oscillations of the genetic oscillator, we measured the time between the first and the second fluorescence maximum for both CFP and YFP fluorescence and used the average. Data were analyzed using IgorPro and MATLAB software.

Fabrication and Design of the Microfluidic Chip. Microfluidic devices were fabricated by standard multilayer soft lithography (41). Details on the design and operation of the chip are provided in *SI Appendix*.

ACKNOWLEDGMENTS. We thank José Garcia and Luis Fidalgo for helpful discussions. This work was supported by École Polytechnique Fédérale de Lausanne and a SystemsX.ch Grant DynamiX-RTD (2008/005).

1. Kim J, Winfree E (2011) Synthetic in vitro transcriptional oscillators. *Mol Syst Biol* 7:465.
2. Montagne K, Plasson R, Sakai Y, Fujii T, Rondelez Y (2011) Programming an in vitro DNA oscillator using a molecular networking strategy. *Mol Syst Biol* 7:466.
3. Loose M, Fischer-Friedrich E, Ries J, Kruse K, Schwille P (2008) Spatial regulators for bacterial cell division self-organize into surface waves in vitro. *Science* 320(5877):789–792.
4. Shimizu Y, et al. (2001) Cell-free translation reconstituted with purified components. *Nat Biotechnol* 19(8):751–755.
5. Noireaux V, Bar-Ziv R, Libchaber A (2003) Principles of cell-free genetic circuit assembly. *Proc Natl Acad Sci USA* 100(22):12672–12677.
6. Ishikawa K, Sato K, Shima Y, Urabe I, Yomo T (2004) Expression of a cascading genetic network within liposomes. *FEBS Lett* 576(3):387–390.

7. Isalan M, Lemerle C, Serrano L (2005) Engineering gene networks to emulate Drosophila embryonic pattern formation. *PLoS Biol* 3(3):e64.
8. Karig DK, Iyer S, Simpson ML, Doktycz MJ (2012) Expression optimization and synthetic gene networks in cell-free systems. *Nucleic Acids Res* 40(8):3763–3774.
9. Shin J, Noireaux V (2012) An E. coli cell-free expression toolbox: Application to synthetic gene circuits and artificial cells. *ACS Synth Biol* 1(1):29–41.
10. Xie Z, Liu SJ, Bleris L, Benenson Y (2010) Logic integration of mRNA signals by an RNAi-based molecular computer. *Nucleic Acids Res* 38(8):2692–2701.
11. Jewett MC, Calhoun KA, Voloshin A, Wuu JJ, Swartz JR (2008) An integrated cell-free metabolic platform for protein production and synthetic biology. *Mol Syst Biol* 4:220.
12. Davidson EA, Meyer AJ, Ellefson JW, Levy M, Ellington AD (2012) An in vitro autogene. *ACS Synth Biol* 1(5):190–196.
13. Shin J, Noireaux V (2010) Study of messenger RNA inactivation and protein degradation in an Escherichia coli cell-free expression system. *J Biol Eng* 4:9.
14. Spirin AS, Baranov VI, Ryabova LA, Ovodov SY, Alakhov YB (1988) A continuous cell-free translation system capable of producing polypeptides in high yield. *Science* 242(4882):1162–1164.
15. Spirin AS (2004) High-throughput cell-free systems for synthesis of functionally active proteins. *Trends Biotechnol* 22(10):538–545.
16. Khnouf R, Beebe DJ, Fan ZH (2009) Cell-free protein expression in a microchannel array with passive pumping. *Lab Chip* 9(1):56–61.
17. Siuti P, Retterer ST, Doktycz MJ (2011) Continuous protein production in nanoporous, picolitre volume containers. *Lab Chip* 11(20):3523–3529.
18. Noireaux V, Libchaber A (2004) A vesicle bioreactor as a step toward an artificial cell assembly. *Proc Natl Acad Sci USA* 101(51):17669–17674.
19. Hansen CL, Sommer MOA, Quake SR (2004) Systematic investigation of protein phase behavior with a microfluidic formulator. *Proc Natl Acad Sci USA* 101(40):14431–14436.
20. Ridgeway WK, Seitaridou E, Phillips R, Williamson JR (2009) RNA-protein binding kinetics in an automated microfluidic reactor. *Nucleic Acids Res* 37(21):e142.
21. Galas J-C, Haghiri-Gosnet AM, Estévez-Torres A (2013) A nanoliter-scale open chemical reactor. *Lab Chip* 13(3):415–423.
22. Niederholtmeyer H, Xu L, Maerkl SJ (2013) Real-time mRNA measurement during an in vitro transcription and translation reaction using binary probes. *ACS Synth Biol* 2(8): 411–417.
23. Karzbrun E, Shin J, Bar-Ziv RH, Noireaux V (2011) Coarse-grained dynamics of protein synthesis in a cell-free system. *Phys Rev Lett* 106(4):048104.
24. Stögbauer T, Windhager L, Zimmer R, Rädler JO (2012) Experiment and mathematical modeling of gene expression dynamics in a cell-free system. *Integr Biol (Camb)* 4(5): 494–501.
25. Elowitz MB, Leibler S (2000) A synthetic oscillatory network of transcriptional regulators. *Nature* 403(6767):335–338.
26. Isaacs FJ, et al. (2004) Engineered riboregulators enable post-transcriptional control of gene expression. *Nat Biotechnol* 22(7):841–847.
27. Anderson JC, Voigt CA, Arkin AP (2007) Environmental signal integration by a modular AND gate. *Mol Syst Biol* 3:133.
28. Banecki B, Wawrzynow A, Puzewicz J, Georgopoulos C, Zylicz M (2001) Structure-function analysis of the zinc-binding region of the Clpx molecular chaperone. *J Biol Chem* 276(22):18843–18848.
29. Stricker J, et al. (2008) A fast, robust and tunable synthetic gene oscillator. *Nature* 456(7221):516–519.
30. Chappell J, Jensen K, Freemont PS (2013) Validation of an entirely in vitro approach for rapid prototyping of DNA regulatory elements for synthetic biology. *Nucleic Acids Res* 41(5):3471–3481.
31. Heyman Y, Buxboim A, Wolf SG, Daube SS, Bar-Ziv RH (2012) Cell-free protein synthesis and assembly on a biochip. *Nat Nanotechnol* 7(6):374–378.
32. Mendell JE, Clements KD, Choat JH, Angert ER (2008) Extreme polyploidy in a large bacterium. *Proc Natl Acad Sci USA* 105(18):6730–6734.
33. Karig DK, Jung S-Y, Srijanto B, Collier CP, Simpson ML (2013) Probing cell-free gene expression noise in femtoliter volumes. *ACS Synth Biol*, 10.1021/sb400028c.
34. Thorsen T, Maerkl SJ, Quake SR (2002) Microfluidic large-scale integration. *Science* 298(5593):580–584.
35. Garcia-Cordero JL, Nembrini C, Stano A, Hubbell JA, Maerkl SJ (2013) A high-throughput nanoimmunoassay chip applied to large-scale vaccine adjuvant screening. *Integr Biol (Camb)* 5(4):650–658.
36. Rockel S, Geertz M, Hens K, Deplancke B, Maerkl SJ (2013) iSLIM: A comprehensive approach to mapping and characterizing gene regulatory networks. *Nucleic Acids Res* 41(4):e52.
37. Tian J, et al. (2004) Accurate multiplex gene synthesis from programmable DNA microchips. *Nature* 432(7020):1050–1054.
38. Fujiwara K, Katayama T, Nomura SM (2013) Cooperative working of bacterial chromosome replication proteins generated by a reconstituted protein expression system. *Nucleic Acids Res* 41(14):7176–7183.
39. Forster AC, Church GM (2006) Towards synthesis of a minimal cell. *Mol Syst Biol* 2:45.
40. Sheff MA, Thorn KS (2004) Optimized cassettes for fluorescent protein tagging in Saccharomyces cerevisiae. *Yeast* 21(8):661–670.
41. Unger MA, Chou HP, Thorsen T, Scherer A, Quake SR (2000) Monolithic microfabricated valves and pumps by multilayer soft lithography. *Science* 288(5463): 113–116.